Diode Laser Spectrum of HCCCN: CN Stretching Band

Koichi Yamada, Regina Best*, and G. Winnewisser

Erstes Physikalisches Institut, Universität zu Köln

Z. Naturforsch. **38 a**, 1296–1308 (1984); received September 1983

The v_2 vibration-rotation band of cyanoacetylene, HCCCN, has been studied by diode laser spectroscopy in the wavenumber region from 2240 cm^{-1} to 2290 cm^{-1}. In addition to the fundamental band we have assigned hot bands arising from $v_7 = 1$, 2, and 3 states and from $v_6 = 1$ state. In these hot bands splittings due to l-type doubling and l-type resonance were clearly observed. The transition wavenumbers were measured precisely, with an estimated error of 0.001 cm^{-1}. Their analysis simultaneously with the microwave data allowed an accurate determination of the band origin $v_0 = 2273.99539(11)$ cm^{-1}, the rotational constant $B' = 4527.4861(28)$ MHz, and the centrifugal distortion constant $D' = 0.53547(43)$ kHz.

I. Introduction

Several of the seven fundamental bands of the linear molecule HC_3N have been measured with high spectral resolution. The C≡C stretching band has been measured by us using a diode laser spectrometer [1, 2], whereas the diode laser spectra of the C≡N stretching band v_2 will be reported in the present work. The first high resolution study of this band was carried out by Mallinson and Fayt [3], who assigned the fundamental and several "hot" bands arising from the $v_7 = 1$ and 2, $v_6 = 1$ and $v_5 = 1$ states. Since this band is of stronger absorption than the v_3 band, many additional hot bands could be observed. However the hot band from the $v_5 = 1$ state has not been identified in the present study. Instead we observed the hot band from the $v_7 = 3$ state. The microwave data [4, 5, 6] were fully utilized to assign the lines and to obtain precise molecular constants.

Since the high resolution rovibrational spectra of HC_3N are of astrophysical interest and since their analysis will allow a precise determination of the equilibrium rotational constant, we intend to measure most of the fundamental bands by diode laser spectroscopy. These data will ultimately be used towards determining the equilibrium structure of HC_3N.

The present work presents an analysis of the C≡N stretching band v_2 and several hot bands associated with it. The $v_7 = 3$ "hot" band is observed in this work for the first time. Measurements for the isotopically substituted molecules, involving D, ^{13}C, and ^{15}N, are also in progress [7].

In the following the vibrational states are presented by the notation $(v_2; v_6, v_7)^l$, where l is the quantum number of the vibrational angular momentum; thus the hot band $v_2 + v_7 - v_7$ will be expressed by $(1; 0, 1)^1 - (0; 0, 1)^1$.

II. Spectra and Analysis

The experimental procedures are identical to the techniques used in our previous diode laser work [1, 2, 8]. The wavenumbers were calibrated by means of the vibration-rotation bands of NNO and $^{13}CO_2$, whose precise line positions were reported by Guelachvili and coworkers [9, 10]. The fringes of a 7.5 cm Ge etalon were used as an interpolation scale and were recorded simultaneously with each spectrum to assure the needed precision. The free spectral range of the etalon (about 0.016 cm^{-1}) was calibrated for every scan. The spectra were measured at room temperature with a 75 cm long glass cell, sealed with two BaF_2 windows. The sample pressure was less than 100 Pa. Therefore the spectral line widths were essentially determined by the Doppler broadening. Figure 1 shows a portion of the recorded spectrum.

1. Fundamental band: $(1; 0, 0)^0 - (0; 0, 0)^0$

For the v_2 fundamental band, the rovibrational lines were assigned from P(86) to R(50). The J assignment was obtained by using the iteration method described in [1]. Thus the very precise, ground vibrational state rotational constant aquainted by

* Present address: Max-Planck-Institut für Quantenoptik, D-8046 Garching, West Germany.

Reprint requests to Dr. Koichi Yamada, I. Physikalisches Institut, Universität zu Köln, 5000 Köln 41.

0340-4811 / 83 / 1200-1296 $ 01.3 0/0. – Please order a reprint rather than making your own copy.

microwave spectroscopy [5] allowed us to find an unique J assignment. The lines were analyzed using a conventional expression

$$\nu = \tilde{G}' + \tilde{B}'[J'(J'+1) - l'^2] - \tilde{D}'[J'(J'+1) - l'^2]^2 - \{\tilde{G}'' + \tilde{B}''[J''(J''+1) - l''^2] - \tilde{D}''[J''(J''+1) - l''^2]^2\}, \quad (1)$$

where $\tilde{G}$, $\tilde{B}$, and $\tilde{D}$ are the effective parameters representing vibrational energy, rotational constants, and quartic centrifugal distortion constants, respectively. For the ν_2 fundamental band, the vibrational angular momentum l' and l'' vanish for both the lower and upper states of the transition. The effective constants, $\nu_0 = \tilde{G}' - \tilde{G}''$, $\tilde{B}'$, and $\tilde{D}'$ were determined by using a least squares fit. The lower state constants, $\tilde{B}''$ and $\tilde{D}''$ were constrained to their microwave values [5]. The observed transitions are listed in Table 1 with the transition wavenumbers calculated on the basis of the constants thus determined.

2. Hot band: $(1;0,1)^1 - (0;0,1)^1$

The strongest hot band observed was identified as the $\Pi - \Pi$ transition of the lowest excited vibrational state, $(0;0,1)^1$. The doubly degenerate Π state, both $(1;0,1)^1$ and $(0;0,1)^1$, are split into two components, e and f, by the l-type doubling interaction. For the P and R branch, which were observed in the present study, the transitions follow the selection rules of e−e and f−f. We have measured the line positions of this band from P(70) to R(72) for both l-type components.

For J larger than ~ 15 the regularly spaced transitions were observed as doublets for both the P and R branch. The observed transition wavenumbers were analyzed for each component separately using the effective expression of (1). Because of the l-type doubling interaction, the doubly degenerate energy level are shifted by the amount of

$$\Delta = \pm [q_t - q_{tJ} J(J+1)] J(J+1)/2, \quad (2)$$

where the constant q_t is the l-type doubling constant and q_{tJ} is its centrifugal correction. The + sign stands for f and − sign for e component. Thus the effective constants in (1) include the effect of this interaction in the form

$$\tilde{G} = G \pm (q_t - q_{tJ} l^2) l^2/2,$$
$$\tilde{B} = B \pm (q_t - 2q_{tJ} l^2)/2,$$
$$\tilde{D} = D \pm q_{tJ}/2. \quad (3)$$

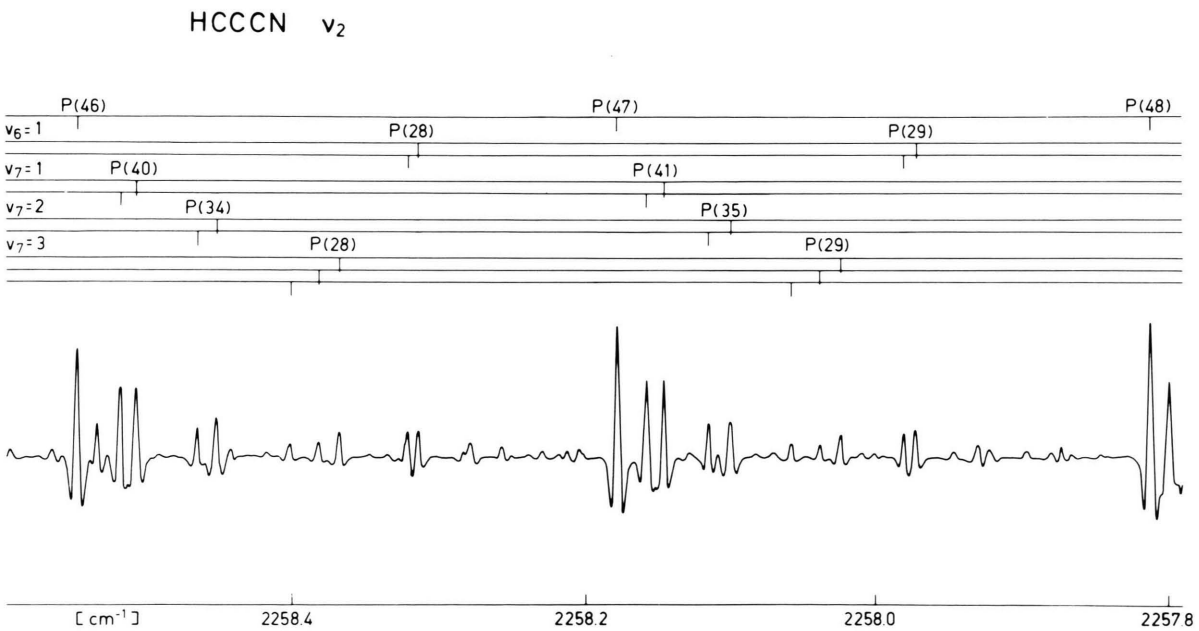

Fig. 1. A portion of the ν_2 band of HCCCN recorded in the present work by frequency modulation. The typical multiplets due to the l-type doubling and l-type resonance interaction confirm the assignment indicated above.

Table 1. Observed transitions in cm^{-1} for the fundamental $(1; 0, 0)^0 - (0; 0, 0)^0$ band of HCCCN [a]

J′ - J″	CALC.	O-C		J′ - J″	CALC.	O-C
85 - 86	2242.6958	0.0013		25 - 26	2265.6386	0.0003
84 - 85	2243.1194	-0.0002		24 - 25	2265.9779	-0.0001
83 - 84	2243.5416	-0.0004		23 - 24	2266.3157	-0.0005
82 - 83	2243.9624	-0.0008				
				14 - 15	2269.2923	-0.0009
79 - 80	2245.2166	0.0002		13 - 14	2269.6159	0.0002
78 - 79	2245.6319	0.0000		12 - 13	2269.9381	0.0002
72 - 73	2248.0945	0.0000		7 - 8	2271.5273	0.0007
71 - 72	2248.5001	-0.0008		6 - 7	2271.8408	0.0004
70 - 71	2248.9043	0.0003		5 - 6	2272.1529	0.0001
69 - 70	2249.3071	0.0002		4 - 5	2272.4636	-0.0005
				3 - 4	2272.7728	-0.0010
66 - 67	2250.5071	0.0004		2 - 3	2273.0806	-0.0008
65 - 66	2250.9043	0.0004		1 - 2	2273.3870	-0.0003
64 - 65	2251.3001	-0.0005		0 - 1	2273.6919	0.0002
63 - 64	2251.6945	-0.0001				
62 - 63	2252.0875	-0.0011		5 - 4	2275.4912	-0.0003
61 - 62	2252.4791	-0.0002		6 - 5	2275.7860	0.0007
60 - 61	2252.8694	-0.0003		7 - 6	2276.0794	0.0003
59 - 60	2253.2582	0.0003		8 - 7	2276.3714	0.0004
58 - 59	2253.6456	0.0003		9 - 8	2276.6619	0.0008
57 - 58	2254.0316	-0.0003		10 - 9	2276.9510	0.0004
56 - 57	2254.4162	0.0005		11 - 10	2277.2386	0.0004
55 - 56	2254.7994	0.0004		12 - 11	2277.5248	-0.0002
54 - 55	2255.1812	0.0001		13 - 12	2277.8095	-0.0002
53 - 54	2255.5616	0.0002				
				31 - 30	2282.6876	-0.0004
48 - 49	2257.4424	-0.0001		32 - 31	2282.9448	0.0000
47 - 48	2257.8143	-0.0001		33 - 32	2283.2006	-0.0006
46 - 47	2258.1848	0.0003		34 - 33	2283.4550	0.0009
45 - 46	2258.5539	0.0022 b		35 - 34	2283.7079	0.0010
44 - 45	2258.9216	-0.0004		36 - 35	2283.9593	0.0006
43 - 44	2259.2879	0.0000		37 - 36	2284.2093	-0.0004
42 - 43	2259.6528	-0.0001				
41 - 42	2260.0163	-0.0002		42 - 41	2285.4375	0.0008
				43 - 42	2285.6788	0.0008
38 - 39	2261.0981	-0.0001		44 - 43	2285.9186	0.0002
37 - 38	2261.4559	-0.0007		45 - 44	2286.1570	0.0018
36 - 37	2261.8123	-0.0010		46 - 45	2286.3939	-0.0004
35 - 36	2262.1672	-0.0006		47 - 46	2286.6294	-0.0005
34 - 35	2262.5208	-0.0007		48 - 47	2286.8634	-0.0003
33 - 34	2262.8729	0.0000		49 - 48	2287.0960	-0.0001
				50 - 49	2287.3271	0.0001
27 - 28	2264.9557	-0.0005		51 - 50	2287.5568	0.0004
26 - 27	2265.2978	0.0003				

[a] The vibrational states are indicated as $(v_2; v_6, v_7)^l$. [b] Not used in the fit.

Table 2. Observed transitions in cm^{-1} for the $(1; 0, 1)^1 - (0; 0, 1)^1$ band of HCCCN [a]

	e - e		f - f	
J' - J"	CALC.	O-C	CALC.	O-C
80 - 81	2242.5552	-0.0004	2242.5414	0.0000
79 - 80	2242.9726	0.0002	2242.9589	-0.0011
78 - 79	2243.3887	-0.0002	2243.3749	0.0013
77 - 78	2243.8033	-0.0003	2243.7896	-0.0005
74 - 75	2245.0389	-0.0006	2245.0253	-0.0006
73 - 74	2245.4480	0.0002	2245.4344	0.0000
72 - 73	2245.8557	0.0007	2245.8422	0.0007
66 - 67	2248.2728	0.0013	2248.2594	0.0012
65 - 66	2248.6708	-0.0001	2248.6574	0.0000
64 - 65	2249.0673	0.0003	2249.0540	-0.0001
60 - 61	2250.6397	0.0009	2250.6265	0.0011
59 - 60	2251.0293	0.0003	2251.0162	0.0020 b
58 - 59	2251.4175	-0.0003	2251.4044	-0.0004
57 - 58	2251.8043	-0.0004	2251.7913	-0.0004
56 - 57	2252.1897	-0.0010	2252.1767	-0.0011
55 - 56	2252.5736	-0.0002	2252.5607	-0.0011
54 - 55	2252.9562	0.0000	2252.9434	0.0002
53 - 54	2253.3374	0.0003	2253.3246	0.0001
52 - 53	2253.7172	0.0004	2253.7044	0.0008
51 - 52	2254.0955	-0.0002	2254.0829	0.0000
50 - 51	2254.4725	-0.0010	2254.4599	-0.0001
49 - 50	2254.8480	0.0002	2254.8355	0.0001
48 - 49	2255.2222	-0.0008	2255.2098	-0.0009
47 - 48			2255.5826	0.0003
42 - 43	2257.4374	-0.0006	2257.4255	0.0001
41 - 42	2257.8016	0.0000	2257.7899	-0.0007
40 - 41	2258.1644	0.0006	2258.1529	0.0002
39 - 40	2258.5259	0.0013	2258.5144	0.0005
38 - 39	2258.8859	-0.0007	2258.8746	-0.0006
37 - 38	2259.2445	0.0001	2259.2333	-0.0002
36 - 37	2259.6016	-0.0001	2259.5906	-0.0004
35 - 36	2259.9574	-0.0007	2259.9465	-0.0007
32 - 33	2261.0161	-0.0005	2261.0057	0.0004
31 - 32	2261.3661	-0.0006	2261.3560	0.0000
30 - 31	2261.7148	-0.0003	2261.7048	-0.0006
29 - 30	2262.0620	-0.0005	2262.0522	-0.0007
28 - 29	2262.4078	-0.0008	2262.3982	-0.0009
27 - 28	2262.7522	0.0001	2262.7428	-0.0002
21 - 22	2264.7884	-0.0005	2264.7804	-0.0006
20 - 21	2265.1228	0.0002	2265.1151	0.0002
19 - 20	2265.4557	0.0004	2265.4483	-0.0001
18 - 19	2265.7872	0.0002	2265.7801	0.0002

Table 2 (continued)

J′ - J″	e - e CALC.	e - e O-C	f - f CALC.	f - f O-C
17 - 18	2266.1173	-0.0003	2266.1104	-0.0003
16 - 17	2266.4460	-0.0008	2266.4394	-0.0013
8 - 9	2269.0235	0.0000	2269.0196	-0.0004
7 - 8	2269.3393	0.0001	2269.3357	0.0005
6 - 7	2269.6536	0.0008	2269.6504	0.0011
5 - 6	2269.9664	-0.0007 b	2269.9637	0.0020 b
2 - 1	2272.4175	0.0000	2272.4181	-0.0006
3 - 2	2272.7174	0.0000	2272.7185	-0.0011
4 - 3	2273.0159	0.0006 b	2273.0174	-0.0009 b
5 - 4	2273.3129	0.0009 b	2273.3149	-0.0011 b
6 - 5	2273.6085	0.0011 b	2273.6110	-0.0014 b
7 - 6	2273.9026	0.0021 b	2273.9056	-0.0009 b
12 - 11	2275.3516	0.0000	2275.3572	0.0008
13 - 12	2275.6371	0.0004	2275.6432	0.0011
14 - 13	2275.9211	-0.0002	2275.9278	0.0001
15 - 14	2276.2036	0.0007	2276.2109	0.0005
16 - 15	2276.4848	0.0004	2276.4926	0.0006
17 - 16	2276.7644	0.0009	2276.7728	0.0012
18 - 17	2277.0427	0.0000	2277.0516	0.0001
19 - 18	2277.3194	0.0001	2277.3290	0.0001
20 - 19	2277.5948	0.0000	2277.6049	0.0001
21 - 20	2277.8687	-0.0008	2277.8794	-0.0008
40 - 39	2282.7969	0.0000		
41 - 40	2283.0418	0.0002	2283.0660	0.0004
42 - 41	2283.2852	0.0008	2283.3101	0.0006
43 - 42	2283.5271	0.0013	2283.5528	0.0007
44 - 43	2283.7676	-0.0008	2283.7940	0.0007
45 - 44	2284.0067	0.0002	2284.0338	0.0003
46 - 45	2284.2443	-0.0006	2284.2722	0.0000
51 - 50	2285.4105	0.0010	2285.4422	0.0015
52 - 51	2285.6394	0.0005	2285.6718	0.0003
53 - 52	2285.8668	0.0006	2285.9000	0.0002
54 - 53	2286.0928	-0.0002	2286.1268	-0.0004
55 - 54	2286.3173	-0.0006	2286.3521	-0.0005
56 - 55	2286.5403	-0.0006	2286.5759	-0.0008
57 - 56	2286.7619	-0.0004	2286.7983	-0.0008
58 - 57	2286.9821	-0.0001	2287.0192	-0.0004
59 - 58	2287.2008	-0.0001	2287.2387	-0.0002
60 - 59	2287.4181	0.0004	2287.4568	0.0013

[a] The vibrational states are indicated by $(v_2; v_6, v_7)^l$. The l-type doubling components are distinguished by e and f.
[b] Not used in the fit.

The constants G, B, and D represent the vibrational energy and the rotational and centrifugal distortion constants in the usual sense.

The parameters in the lower state, $(0;0,1)^1$, where determined by analyzing the microwave data reported by Mallinson and de Zafra [4] together with Creswell's new measurements [6]. They were constrained to these values in the final fit. The observed transitions and calculated wavenumbers are listed in Table 2.

3. Hot band: $(1;0,2)^{0,2}-(0;0,2)^{0,2}$

The second excited state of the bending vibration in a linear molecule is triply degenerate. The anharmonic potential removes this degeneracy and splits the level into an $l=0$ (Σ) state and two $l=2$ (Δ) states. The doubly degenerate Δ state is further separated by l-type resonance into e and f components. The vibration-rotation energy of these three levels are given analytically as

$$E(\Sigma,\Delta e)=\{E_0+E_2\pm[(E_2-E_0)^2+8W_{02}^2]^{1/2}\}/2,$$

and

$$E(\Delta f) \quad =E_2, \tag{4}$$

where

$$E_0/hc=G+BJ(J+1)-D[J(J+1)]^2,$$

$$E_2/hc=G+4x_{l_7l_7}+(B+4\gamma_{ll})\cdot[J(J+1)-4]-D[J(J+1)-4]^2, \tag{5}$$

and

$$W_{02}/hc \;=[q_t-q_{tJ}J(J+1)]\cdot\{J(J+1)[J(J+1)-2]/2\}^{1/2}.$$

Here G is the vibrational energy without the contribution from the vibrational angular momentum. This contribution is explicitly represented by the term $x_{l_7l_7}$ in the second equation of (5). The l dependence of the rotational constant is taken into account by the term γ_{ll}.

The transition wavenumbers were calculated applying (4) for both the $(1;0,2)^{0,2}$ and $(0;0,2)^{0,2}$ states. From the present infrared data the parameters in the upper state, $(1;0,2)^{0,2}$, were determined by least-squares fittings whereas the lower state constants were fixed at the microwave values [4, 6]. The microwave data alone did not allow us to determine the sign of $(x'_{l_7l_7}-B'')$ [5]. However the present analysis of the infrared spectrum confirmed definitely that the sign of this value is positive. The observed transitions are listed in Table 3 together with the calculated wavenumbers.

4. Hot band: $(1;0,3)^{1,3}-(0;0,3)^{1,3}$

The third excited states of a bending vibration of a linear molecule is composed of the $l=1$ (Π) and $l=3$ (Φ) state. The degenerate Π state splits into two components, e and f, and the Φ state also splits into an e and f state by l-type doubling and l-type resonance interactions. In the present study the $\Pi-\Pi$ band was observed from P(55) to R(32), and the $\Phi-\Phi$ band from P(70) to R(61). The line splittings due to the l-type doubling were observed in the $\Pi-\Pi$ band R-branch transitions at high J values. In the P branch the splitting was not resolved for the J values observed. For the $\Phi-\Phi$ band, the splitting due to the l-type resonance was too small to be resolved.

Since the microwave data of the $(0;0,3)^{1,3}$ state [4, 6] show that this state is perturbed by another vibrational state, presumably by the $v_5=1$ state, we have analyzed this hot band by applying only the effective expression of (1). The effective parameters for both upper and lower states were determined from the present infrared data only. The observed transitions are listed in Table 4 together with the calculated wavenumbers. The microwave data for the $(0;0,3)^{1,3}$ states [4, 6] were used only to confirm the assignment.

5. Hot band: $(1;1,0)^1-(0;1,0)^1$

The $\Pi-\Pi$ hot band arising from the first excited state of the second lowest bending vibration was observed from P(70) to R(79). The analysis was carried out in exactly the same manner as for the hot band $(1;0,1)^1-(0;0,1)^1$. The splittings due to the l-type doubling were observed for high J transitions. The observed transitions are listed in Table 5 together with the calculated wavenumbers.

III. Results

The obtained constants for the fundamental $(1;0,0)^0-(0;0,0)^0$ and the hot bands $(1;0,1)^1-(0;0,1)^1$, $(1;0,2)^{0,2}-(0;0,2)^{0,2}$, and $(1;1,0)^1-(0;1,0)^1$ are summarized in Table 6. For the $\Pi-\Pi$ hot bands the constants were obtained from the

Table 3. Observed transitions in cm^{-1} for the $(1; 1, 0)^1 - (0; 1, 0)^1$ band of HCCCN [a]

	e - e		f - f	
J′ - J″	CALC.	O-C	CALC.	O-C
69 - 70	2242.6872	0.0003	2242.6683	-0.0001
68 - 69	2243.0883	0.0006	2243.0696	0.0010
67 - 68	2243.4879	-0.0001	2243.4695	0.0004
66 - 67	2243.8861	0.0004	2243.8680	-0.0004
63 - 64	2245.0725	-0.0002	2245.0553	0.0003
62 - 63	2245.4652	-0.0003		
55 - 56	2248.1750	-0.0007	2248.1601	0.0011
54 - 55	2248.5566	-0.0010	2248.5419	-0.0012
53 - 54	2248.9367	0.0002	2248.9223	0.0001
52 - 53	2249.3155	0.0003	2249.3014	-0.0003
48 - 49	2250.8165	-0.0003	2250.8036	-0.0001
47 - 48	2251.1883	0.0004	2251.1756	-0.0006
46 - 47	2251.5586	0.0003	2251.5462	0.0005
45 - 46	2251.9276	-0.0013	2251.9155	-0.0013
44 - 45	2252.2951	-0.0012	2252.2833	-0.0015
43 - 44	2252.6613	-0.0012	2252.6498	-0.0021 b
42 - 43	2253.0260	-0.0005	2253.0148	0.0000
41 - 42	2253.3894	-0.0001	2253.3785	-0.0002
40 - 41	2253.7513	-0.0003	2253.7407	-0.0005
39 - 40	2254.1119	-0.0003	2254.1015	0.0001
37 - 38	2254.8288	-0.0001	2254.8190	0.0001
35 - 36	2255.5400	0.0000	2255.5308	-0.0003
30 - 31	2257.2935	0.0000	2257.2857	-0.0002
29 - 30	2257.6400	0.0001	2257.6324	0.0003
28 - 29	2257.9851	0.0001	2257.9778	0.0005
27 - 28	2258.3287	0.0010	2258.3217	0.0008
26 - 27	2258.6710	-0.0007	2258.6642	-0.0008
25 - 26	2259.0118	0.0003	2259.0053	0.0001
24 - 25	2259.3512	-0.0004	2259.3450	-0.0001
23 - 24	2259.6892	0.0003	2259.6833	-0.0002
22 - 23	2260.0258	0.0002		
19 - 20	2261.0272	0.0000	2261.0223	0.0003
17 - 18	2261.6876	0.0002	2261.6833	-0.0002
16 - 17	2262.0158	-0.0008	2262.0117	-0.0008
15 - 16	2262.3424	-0.0009	2262.3386	-0.0009
14 - 15	2262.6677	-0.0013	2262.6642	-0.0016
13 - 14	2262.9916	-0.0028 b	2262.9883	0.0005 b
7 - 8	2264.9050	-0.0010 b	2264.9032	0.0008 b
6 - 7	2265.2189	-0.0002 b	2265.2174	0.0013 b

Table 3 (continued)

J′ - J″	e - e CALC.	e - e O-C	f - f CALC.	f - f O-C
5 - 6	2265.5314	0.0005 b	2265.5302	0.0017 b
4 - 5	2265.8425	-0.0004 b	2265.8415	0.0006 b
3 - 4	2266.1522	-0.0006	2266.1514	0.0002
5 - 4	2268.8752	0.0013 b	2268.8766	-0.0001 b
6 - 5	2269.1706	-0.0003 b	2269.1722	-0.0019 b
7 - 6	2269.4646	0.0020 b	2269.4664	0.0002 b
8 - 7	2269.7572	0.0021 b	2269.7592	0.0001 b
14 - 13	2271.4827	0.0010	2271.4860	0.0008
15 - 14	2271.7652	0.0007	2271.7688	0.0004
16 - 15	2272.0464	0.0000	2272.0502	0.0010
17 - 16			2272.3301	0.0000
18 - 17	2272.6044	-0.0005	2272.6086	-0.0001
19 - 18	2272.8812	-0.0001	2272.8857	-0.0009
20 - 19	2273.1566	-0.0004	2273.1613	-0.0005
21 - 20	2273.4306	0.0002	2273.4355	0.0006
22 - 21	2273.7032	0.0011	2273.7083	0.0008
28 - 27	2275.3084	0.0001	2275.3147	0.0005
29 - 28	2275.5709	0.0006	2275.5775	0.0004
30 - 29	2275.8320	0.0010	2275.8387	0.0011
31 - 30	2276.0917	0.0008	2276.0986	0.0006
32 - 31	2276.3499	0.0008	2276.3570	0.0006
33 - 32	2276.6066	0.0007	2276.6140	0.0007
34 - 33	2276.8620	0.0001	2276.8695	0.0002
35 - 34	2277.1159	0.0009	2277.1236	-0.0001
36 - 35	2277.3683	-0.0003	2277.3762	-0.0002
59 - 58	2282.7773	-0.0004	2282.7895	-0.0013
60 - 59	2282.9951	-0.0003	2283.0075	0.0000
61 - 60	2283.2115	0.0003	2283.2241	0.0002
62 - 61	2283.4265	-0.0008	2283.4392	0.0004
63 - 62	2283.6400	0.0009	2283.6529	0.0005
64 - 63	2283.8520	0.0011	2283.8652	0.0004
65 - 64	2284.0627	-0.0003	2284.0760	0.0003
72 - 71	2285.4964	0.0011	2285.5111	0.0001
73 - 72	2285.6955	0.0016	2285.7103	0.0010
76 - 75	2286.2838	-0.0003	2286.2993	-0.0008
77 - 76	2286.4771	-0.0004	2286.4927	-0.0006
78 - 77	2286.6689	-0.0004	2286.6847	-0.0008
79 - 78			2286.8752	0.0008
80 - 79	2287.0481	-0.0011	2287.0643	-0.0001

[a, b] For footnotes see Table 2.

Table 4. Observed transitions in cm^{-1} for the $(1; 0, 2)^{0,2}-(0; 0, 2)^{0,2}$ band of HCCCN [a]

	0 - 0		2e - 2e		2f - 2f	
J′ - J″	CALC.	O-C	CALC.	O-C	CALC.	O-C
74 - 75	2242.8203	-0.0004	2242.7927	-0.0004	2242.8015	-0.0001
73 - 74	2243.2301	0.0005	2243.2026	-0.0003	2243.2114	-0.0008
72 - 73	2243.6385	0.0004	2243.6112	0.0002	2243.6198	0.0004
68 - 69	2245.2582	0.0005	2245.2315	0.0005	2245.2397	0.0000
60 - 61	2248.4307	-0.0012	2248.4057	-0.0019 b	2248.4128	-0.0012
59 - 60	2248.8210	0.0000	2248.7963	-0.0002	2248.8031	-0.0003
58 - 59	2249.2099	0.0003	2249.1854	0.0005	2249.1921	0.0003
54 - 55	2250.7514	0.0005	2250.7280	0.0006	2250.7341	0.0003
53 - 54	2251.1332	0.0005	2251.1102	-0.0003	2251.1161	-0.0001
52 - 53	2251.5137	-0.0002	2251.4910	-0.0002	2251.4967	0.0003
51 - 52	2251.8927	-0.0006	2251.8704	-0.0011	2251.8758	-0.0004
50 - 51	2252.2704	-0.0013	2252.2483	-0.0015	2252.2536	-0.0013
49 - 50	2252.6466	0.0011	2252.6249	-0.0009	2252.6300	-0.0004
48 - 49	2253.0215	-0.0005	2253.0001	0.0009	2253.0050	0.0009
47 - 48	2253.3949	0.0007	2253.3738	0.0003	2253.3786	-0.0003
46 - 47	2253.7670	-0.0003	2253.7462	-0.0002	2253.7508	0.0002
45 - 46	2254.1376	0.0000	2254.1172	-0.0002	2254.1215	0.0001
44 - 45	2254.5068	-0.0005	2254.4867	0.0018 b	2254.4909	-0.0024 b
43 - 44	2254.8746	-0.0004	2254.8549	0.0002 b	2254.8588	0.0009 b
42 - 43	2255.2410	0.0003				
41 - 42	2255.6060	0.0003				
36 - 37	2257.4099	0.0002	2257.3924	0.0010 b	2257.3951	-0.0017 b
35 - 36	2257.7664	-0.0012	2257.7492	0.0011 b	2257.7518	-0.0015 b
34 - 35	2258.1215	-0.0006	2258.1047	0.0011 b	2258.1070	-0.0012 b
33 - 34	2258.4753	-0.0006	2258.4587	0.0020 b	2258.4609	-0.0002 b
32 - 33	2258.8276	-0.0001	2258.8112	0.0009 b	2258.8133	-0.0012 b
31 - 32	2259.1785	0.0007	2259.1624	0.0017 b	2259.1643	-0.0002 b
30 - 31	2259.5280	0.0006	2259.5122	0.0004 b	2259.5139	-0.0013 b
29 - 30	2259.8760	-0.0001	2259.8605	0.0009 b	2259.8621	-0.0007 c
26 - 27	2260.9118	-0.0003	2260.8969	0.0000 c	2260.8981	-0.0012 c
25 - 26	2261.2542	-0.0009	2261.2395	0.0005 c	2261.2407	-0.0007 c
24 - 25	2261.5952	-0.0004	2261.5807	-0.0002 c	2261.5818	-0.0013 c
23 - 24	2261.9348	-0.0013	2261.9205	-0.0008 c	2261.9214	-0.0017 c
22 - 23	2262.2730	-0.0010	2262.2589	-0.0003 c	2262.2597	-0.0011 c
21 - 22	2262.6098	-0.0003	2262.5958	0.0005 c	2262.5965	-0.0002 c
20 - 21	2262.9451	-0.0006	2262.9313	-0.0005 c	2262.9319	-0.0011 c
14 - 15	2264.9274	0.0001	2264.9142	0.0001 c	2264.9144	-0.0001 c
13 - 14	2265.2528	0.0003	2265.2397	0.0005 c	2265.2399	0.0003 c
12 - 13	2265.5767	0.0007	2265.5637	0.0008 c	2265.5639	0.0006 c
11 - 12	2265.8993	-0.0002	2265.8863	0.0002 c	2265.8865	0.0000 c
10 - 11	2266.2204	-0.0002	2266.2075	-0.0004 c	2266.2076	-0.0005 c

Table 4 (continued)

J′ - J″	0 - 0 CALC.	0-C		2e - 2e CALC.	0-C		2f - 2f CALC.	0-C	
6 - 5	2271.4609	0.0009		2271.4482	0.0003	c	2271.4481	0.0004	c
7 - 6	2271.7563	0.0005		2271.7435	0.0012	c	2271.7435	0.0012	c
8 - 7	2272.0502	0.0004		2272.0375	0.0003	c	2272.0374	0.0004	c
9 - 8	2272.3426	-0.0001		2272.3300	0.0002	c	2272.3299	0.0003	c
10 - 9	2272.6337	-0.0006		2272.6210	-0.0002	c	2272.6209	-0.0001	c
11 - 10	2272.9232	-0.0006		2272.9107	-0.0007	c	2272.9105	-0.0005	c
12 - 11	2273.2113	-0.0005		2273.1989	-0.0002	c	2273.1987	0.0000	c
13 - 12	2273.4980	0.0001		2273.4857	0.0004	c	2273.4854	0.0007	c
14 - 13	2273.7832	0.0008		2273.7710	0.0004	c	2273.7707	0.0007	c
20 - 19	2275.4641	0.0003		2275.4530	-0.0005	c	2275.4522	0.0003	c
21 - 20	2275.7391	0.0003		2275.7283	0.0003	c	2275.7274	0.0012	c
22 - 21	2276.0127	0.0000		2276.0022	-0.0001	c	2276.0011	0.0010	c
23 - 22	2276.2848	0.0005		2276.2747	-0.0001	b	2276.2734	0.0012	b
24 - 23	2276.5555	0.0011		2276.5458	-0.0004	b	2276.5443	0.0011	b
25 - 24	2276.8247	0.0007		2276.8154	-0.0003	b	2276.8137	0.0014	b
26 - 25	2277.0924	0.0001							
27 - 26	2277.3587	-0.0003		2277.3503	-0.0008	b			
28 - 27	2277.6235	0.0002		2277.6157	-0.0010	b	2277.6133	0.0014	b
49 - 48	2282.8448	0.0005		2282.8590	-0.0002		2282.8460	-0.0007	
50 - 49	2283.0773	0.0012		2283.0930	-0.0001		2283.0792	-0.0007	
51 - 50				2283.3256	0.0009				
52 - 51	2283.5377	0.0011					2283.5414	0.0015	
53 - 52				2283.7865	0.0006				
54 - 53	2283.9922	0.0006		2284.0147	0.0004		2283.9977	0.0011	
55 - 54	2284.2173	-0.0028	b	2284.2416	-0.0007		2284.2237	-0.0004	
61 - 60	2285.5368	0.0004		2285.5726	0.0017		2285.5491	0.0009	
62 - 61	2285.7516	0.0005					2285.7649	0.0005	
63 - 62	2285.9649	-0.0004		2286.0048	0.0008		2285.9793	0.0000	
64 - 63	2286.1768	-0.0006		2286.2187	-0.0004		2286.1922	-0.0002	
66 - 65	2286.5962	-0.0014		2286.6422	-0.0010		2286.6137	0.0008	

[a] The vibrational states are indicated as $(v_2; v_6, v_7)^l$. The transitions of $\Sigma-\Sigma$ band are listed in the column of 0−0, and of $\Delta-\Delta$ band are in the column of 2−2, where l-type components are distinguished by e and f.
[b] Not used in the fit.
[c] Unresolved l-doublets which were less weighted in the fit by factor of 0.5 than the others.

effective parameters using (3). The band origins v_0 for the $\Pi-\Pi$ hot bands contain a contribution of the $x_{l_t l_t}$ term, and the rotational constants for the Π states contain a small contribution from the γ_{ll} term. From the band origins listed in Table 7 we could determine several linear combinations of harmonic and anharmonic parameters which appear in the vibrational energy expression:

$$G^0 = \sum_i \omega_i^0 v_i + \sum_{i \leqq j} x_{ij}^0 v_i v_j + \sum_{i \leqq j \leqq k} y_{ijk}^0 v_i v_j v_k + \sum_{i \leqq j} \left(x_{lilj} + \sum_k x_{lilj}^{(k)} v_k\right) l_i l_j . \quad (6)$$

This equation is slightly different from that used in the previous work for the v_3 band (Equation (2) in [2]): the contribution from the rotational energy, $-Bl^2$, is not included in G^0 in the above equation. We reserve the notation g_{ll} for the value which includes that. The values thus obtained are listed in Table 8.

For the $(1; 0, 3)^{1,3}-(0; 0, 3)^{1,3}$ band only effective parameters were obtained, which are summarized in Table 9. The complete analysis, which includes higher order interactions, is in progress and will be published elsewhere.

Table 5. Observed transitions in cm^{-1} for the $(1; 0, 3)^1 - (0; 0, 3)^1$ band of HCCCN [a]

	e - e		f - f	
J′ - J″	CALC.	O-C	CALC.	O-C
54 - 55	2248.5637	0.0019	2248.5650	0.0006
53 - 54	2248.9471	-0.0012	2248.9465	-0.0006
49 - 50	2250.4663	0.0001		
47 - 48	2251.2171	-0.0009		
42 - 43	2253.0691	-0.0027 b	2253.0541	-0.0041 b
41 - 42	2253.4351	-0.0004	2253.4195	-0.0013
40 - 41	2253.7997	-0.0005	2253.7835	0.0012
39 - 40	2254.1629	-0.0015		
38 - 39	2254.5247	0.0003		
37 - 38	2254.8850	0.0004		
30 - 31	2257.3670	-0.0019 b	2257.3482	-0.0017
29 - 30	2257.7159	0.0014	2257.6972	0.0009
28 - 29	2258.0633	0.0009	2258.0447	-0.0005
27 - 28	2258.4093	0.0014	2258.3909	0.0009
26 - 27	2258.7538	0.0001	2258.7357	0.0001
25 - 26	2259.0969	0.0013	2259.0791	0.0005
24 - 25	2259.4386	-0.0005	2259.4211	-0.0005
23 - 24	2259.7789	0.0002	2259.7617	0.0010
22 - 23			2260.1010	0.0006
19 - 20	2261.1257	-0.0001	2261.1103	0.0010
18 - 19			2261.4440	-0.0014
17 - 18	2261.7905	-0.0013	2261.7763	-0.0012
16 - 17	2262.1208	-0.0010	2262.1071	0.0001
15 - 16	2262.4497	-0.0005	2262.4366	-0.0004
14 - 15	2262.7771	-0.0008	2262.7647	0.0006
7 - 8	2265.0290	0.0001	2265.0217	-0.0014
6 - 7	2265.3450	0.0005	2265.3385	0.0011
14 - 13	2271.6489	0.0003	2271.6624	0.0008
15 - 14	2271.9332	0.0003	2271.9478	0.0006
16 - 15	2272.2161	-0.0006	2272.2317	-0.0004
17 - 16	2272.4975	0.0003	2272.5142	-0.0003
19 - 18	2273.0559	-0.0006		
20 - 19	2273.3330	0.0032 b	2273.3531	-0.0003
21 - 20	2273.6085	0.0010		
22 - 21			2273.9052	-0.0005
30 - 29			2276.0554	0.0007
31 - 30			2276.3177	0.0001
33 - 32	2276.8008	-0.0007	2276.8379	-0.0004
34 - 33	2277.0573	0.0000		
35 - 34	2277.3122	0.0004		

[a, b] For footnotes see Table 2.

Table 6. Observed transitions in cm^{-1} for the $(1;0,3)^3-(1;0,3)^3$ band of HCCCN [a]

J′ - J″	CALC.	O-C	J′ - J″	CALC.	O-C
69 - 70	2242.6214	-0.0006	7 - 8	2265.0020	0.0007
68 - 69	2243.0251	0.0010			
67 - 68	2243.4274	0.0007	4 - 5	2265.9469	0.0002
66 - 67	2243.8283	0.0002			
			5 - 4	2269.0036	-0.0014
62 - 63	2245.4182	-0.0006			
61 - 62	2245.8122	-0.0012	7 - 6	2269.5977	-0.0005
			8 - 7	2269.8926	0.0007
55 - 56	2248.1470	-0.0002			
54 - 55	2248.5312	0.0000	14 - 13	2271.6321	0.0010
53 - 54	2248.9141	0.0001	15 - 14	2271.9170	0.0002
			16 - 15	2272.2004	-0.0004
49 - 50	2250.4315	-0.0010	17 - 16	2272.4824	0.0000
48 - 49	2250.8073	0.0002	18 - 17	2272.7630	-0.0007
47 - 48	2251.1818	0.0000	19 - 18	2273.0422	-0.0006
46 - 47	2251.5548	0.0001	20 - 19	2273.3199	0.0004
			21 - 20	2273.5961	0.0004
42 - 43	2253.0330	0.0000	22 - 21	2273.8710	0.0016
41 - 42	2253.3990	0.0006			
40 - 41	2253.7636	0.0006	29 - 28	2275.7546	0.0000
39 - 40	2254.1268	0.0006	30 - 29	2276.0179	0.0004
			31 - 30	2276.2798	-0.0001
30 - 31	2257.3322	-0.0001			
29 - 30	2257.6813	0.0003	33 - 32	2276.7993	0.0008
28 - 29	2258.0289	0.0005	34 - 33	2277.0568	0.0005
27 - 28	2258.3752	0.0009	35 - 34	2277.3130	-0.0004
26 - 27	2258.7200	-0.0002	36 - 35	2277.5677	-0.0004
25 - 26	2259.0635	0.0000	37 - 36	2277.8210	-0.0017
24 - 25	2259.4055	-0.0003			
23 - 24	2259.7461	0.0002	58 - 57	2282.8072	-0.0007
22 - 23	2260.0852	-0.0002	59 - 58	2283.0288	0.0002
			60 - 59	2283.2490	0.0009
18 - 19	2261.4277	-0.0013	61 - 60	2283.4677	-0.0009
17 - 18	2261.7597	0.0000	62 - 61	2283.6850	0.0005
16 - 17	2262.0904	-0.0008			
15 - 16	2262.4196	-0.0005			

[a] For footnote see Table 1.

Table 7. Molecular constants of HCCCN obtained from the ν_2 fundamental and hot bands [a]

		$(1;0,0)^0-(0;0,0)^0$	$(1;0,1)^1-(0;0,1)^1$	$(1;1,0)^1-(0;1,0)^1$	$(1;0,2)^{0,2}-(0;0,2)^{0,2}$
ν_0	[cm^{-1}]	2273.99539(11)	2271.81254(10)	2267.37605(12)	2269.65867(12)
B'	[MHz]	4527.4861(28)	4541.9747(25)	4536.9603(32)	4556.4545(33)
B''		4549.0579[b]	4563.5130[c]	4558.3142[c]	4577.9672[c]
D'	[kHz]	0.53547(43)	0.56026(43)	0.55091(55)	0.58575(56)
D''		0.54311[b]	0.56765[c]	0.55456[c]	0.59329[c]
q_t'	[MHz]	–	6.6638(50)	3.5606(65)	6.6704(59)
q_t''		–	6.5382[c]	3.5820[c]	6.5595[c]
q_{tJ}'	[Hz]	–	20.29(86)	0.42(110)	25.0(12)
q_{tJ}''		–	15.69[c]	1.62[c]	21.99[c]
$\gamma'_{lt\,lt}$	[kHz]	–	[d]	[d]	− 9.50(71)
$\gamma''_{lt\,lt}$		–			− 13.031[c]
$x'_{lt\,lt}$	[cm^{-1}]	–	[e]	[e]	0.71662(4)
$x''_{lt\,lt}$		–			0.72054[c]

[a] The bands are indicated as $(v_2';v_6',v_7')^{l'}-(v_2'';v_6'',v_7'')^{l''}$. The numbers in the parentheses corresponds to one standard deviation in the unit of the last digit quoted. The conversion factor of $1\ cm^{-1} = 29\,979.2458$ MHz was used in the calculations.
[b] Fixed at the values given in [5].
[c] Fixed at the values obtained from the preliminary analysis of the microwave data (see text).
[d] Included in the rotational constants.
[e] Included in the band origin.

Table 8. Anharmonic constants derived from the present analysis

$\omega_2^0 + x_{22}^0 + y_{222}^0 =$	2273.99539(11) cm^{-1}
$x_{27}^0 + y_{227}^0 =$	− 2.18950(37) cm^{-1}
$y_{277}^0 =$	0.01057(18) cm^{-1}
$x_{l_7 l_7}^{(2)} =$	− 0.00392 (4) cm^{-1}
$x_{26}^0 + y_{226}^0 + y_{266}^0 + x_{l_7 l_7}^{(2)} =$	− 6.61934(17) cm^{-1}

The present results agree very well with those of Mallinson and Fayt [3], except that we could not identify the hot band arising from the $v_5 = 1$ state. Since we have succeeded to assign the hot band from the $v_7 = 3$ state, for which the Boltzmann factor is almost equal to that for the $v_5 = 1$ state, we should have observed the lines of the hot band arrising from it. Probably the lines of this band are obscured by the overlapp of other lines in the region of the present measurement.

Table 9. Effective parameters for $(1; 0, 0)^{1,3} - (0; 0, 3)^{1,3}$ band of HCCCN [a]

l-subband	$\tilde{\nu}_0$ [cm^{-1}]	$\tilde{B}'$ / $\tilde{B}''$ [MHz]	$\tilde{D}'$ / $\tilde{D}''$ [kHz]
1e−1e	2267.51605(34)	4564.60(27) 4586.12(26)	1.04(14) 0.98(13)
1f−1f	2267.51565(37)	4578.38(30) 4599.72(29)	1.46(18) 1.49(17)
3e, f−3e, f	2267.48669(18)	4571.100(88) 4592.546(85)	0.465(15) 0.476(14)

[a] For footnote see Table 7.

Acknowledgement

We are grateful to Dr. R. A. Creswell for sending us his latest microwave and millimeter wave data prior to publication. This work has been supported in part by the Deutsche Forschungsgemeinschaft – SFB-131 – Radioastronomie.

[1] K. Yamada, R. Schieder, G. Winnewisser, and A. W. Mantz, Z. Naturforsch. **35a,** 690 (1980).
[2] K. Yamada and G. Winnewisser, Z. Naturforsch. **36a,** 23 (1981).
[3] P. D. Mallinson and A. Fayt, Mol. Phys. **32,** 473 (1976).
[4] P. D. Mallinson and R. L. de Zafra, Mol. Phys. **36,** 827 (1978).
[5] R. A. Creswell, G. Winnewisser, and M. C. L. Gerry, J. Mol. Spectrosc. **65,** 420 (1977).
[6] R. A. Creswell, private communication.
[7] K. Yamada and G. Winnewisser, J. Mol. Spectrosc. **88,** 207 (1981).
[8] K. Yamada and G. Winnewisser, Z. Naturforsch. **36a,** 1052 (1981).
[9] C. Amiot and G. Guelachvili, J. Mol. Spectrosc. **59,** 171 (1976).
[10] G. Guelachvili, J. Mol. Spectrosc. **79,** 72 (1980).